
DISLOCATION STRUCTURE AND “DISLOCATION” PHOTOLUMINESCENCE IN CADMIUM TELLURIDE CRYSTALS

V.A. BOYKO, N.I. TARBAEV, G.A. SHEPELSKII

UDC 538
©2007

V. Lashkarev Institute of Semiconductor Physics, Nat. Acad. Sci. of Ukraine
(42, Nauky Prosp., Kyiv 01650, Ukraine; e-mail: v_boyko@hotmail.ru)

The generation of dislocations in CdTe and Cd(Zn)Te crystals gives rise to the appearance of new bands — “dislocation” photoluminescence — in the spectra of radiative recombination. Comparing the spatial distribution of the radiation intensity for various radiation bands for (111) and (001) faces with the crystallographic structure of dislocations, we identified the types of defects responsible for the “dislocation” photoluminescence.

1. Introduction

Cadmium telluride is widely used in various fields of solid-state optoelectronics. For example, CdTe represents a basic material of substrates for highly sensitive photodetectors of infrared radiation based on $\text{Cd}_x\text{Hg}_{1-x}\text{Te}$ epitaxial layers. In addition, cadmium telluride is widely used as a material for electro-optical modulators, ionizing-radiation detectors, optical switches, and solar batteries as well as an active element of ultrasonic wave detectors.

A practical use of CdTe makes strict demands to the degree of homogeneity of the structural, optical, and electric properties of the material. The indicated properties are essentially influenced by crystalline defects of different nature; in particular, the important role is played by one-dimensional structural defects — dislocations. The origination of dislocations in CdTe crystals and the generation of point defects during the motion of dislocations in the crystal lattice affect essentially the physical parameters of the crystal as well as their stability. However, till recently, the investigations of the influence of “fresh”, i.e., non-growth dislocations on the physical properties of CdTe were of limited character. At the same time, cadmium telluride belongs to very plastic, that is, hard-to-machine materials. For example, at room temperature, dislocations can be easily introduced into CdTe crystals due to even inessential mechanical impacts. Moreover, the plasticity range of CdTe covers the region of much lower temperatures, practically down to $T=100$ K [1–3]. Thus, in the course of various standard technological

operations necessary for the production of semiconductor devices, such as the mechanical treatment of a surface, thermal processing, ion implantation, etc., a considerable quantity of dislocations and other defects of the deformation origin can be generated in the active part of an element. In CdTe-based devices, they can also be formed during the necessary operations of thermocycles. Such defects can essentially influence the characteristics of devices and the processes of their degradation.

Among various techniques used in the investigation of the processes of generation of defects and the identification of their types in semiconductors, a special place is held by the photoluminescence (PL) and cathodoluminescence (CD) methods due to their high sensitivity and resolving power. These methods include both the spectral and spatial-resolution analyses of the emission from crystals and appear to be especially efficient at low temperatures.

In works [4–7], it was shown that the generation of dislocations in CdTe crystals gives rise to the appearance of a characteristic radiation band — “dislocation” luminescence (DL) — in the spectra of recombination radiation of CdTe. At $T=4.2\div 10$ K, the spectral maximum of the DL band is located at 1.480 meV (841 nm). In most detail, DL in CdTe was studied in [4,5]. The comparison of the crystallographic structure of dislocations with the data obtained from CL measurements allowed one to conclude that the characteristic DL in CdTe was associated with electronic states of 60-degree dislocations that bounded the semiareas surrounded by tellurium atoms — $\text{Te}(g)$ dislocations.

In the present paper, it is shown that the generation and the motion of dislocations actually cause much more complicated changes in the spectra of recombination radiation of CdTe crystals than it was considered earlier. We have discovered two series of characteristic bands of “dislocation” PL and identified the types of defects responsible for the both indicated series.

2. Experimental Technique

We investigated the parallel-sided plates of a specially undoped high-resistance monocrystal of cadmium telluride grown by the Bridgman technique. The plates were cut off with orientation along the {001} and {111} planes, grinded, and mechanically polished. In order to ultimately delete the surface defective layer, the samples were chemically polished in a Br solution in methanol. The density of growth dislocations in the samples didn't exceed $5 \times 10^5 \text{ cm}^{-2}$. In order to create an additional structure of fresh dislocations, we performed single pricks with an indenter or scribed the sample, i.e. marked its surface with rectilinear scratches applied with an indenter. The indentation of the surface was performed using a PMT-3 setup for the microhardness testing with the help of a Vickers indenter at a load of 10 g, a constant rate of $15 \mu\text{m/s}$, and room temperature. After that, the samples were at once inserted into a cryostat and rapidly cooled. In the course of the measurements, the sample was directly in cryogenic liquid.

The PL was excited with the radiation of a helium-neon laser 40 mW in power. The PL spectra in the temperature range $T=4.2 \div 150 \text{ K}$ were recorded with the help of a KSVU-2 spectral complex at a reciprocal linear dispersion of 2.6 nm/mm. The spatial resolving power was determined by focusing the exciting laser radiation onto a spot $30 \mu\text{m}$ in diameter.

In order to obtain the profiles of the spatial distribution of the PL intensity, the face of the sample was located in parallel to the entrance slit of the spectral device. Thus, when we shifted the sample along the plane of the face normally to the optical axis of a monochromator, the region of the sample excitation was always at this axis. As a result, the focused radiation from the sample (PL) was always located at the entrance slit of the monochromator. The profiles of the spatial distribution of the intensity for various PL bands were recorded by the repeated scanning of the same region of the surface.

3. Experimental Results and Their Discussion

PL spectra. In the PL spectra obtained in the regions of indentation of the surface of CdTe crystals, there appear the radiation bands (Fig. 1) absent in the initial samples. New radiation bands in the vicinity of 1.54 eV (805–806 nm) are observed in the low-temperature region $T < 100 \text{ K}$. In this case, there usually arise two close bands. The best temperature for the

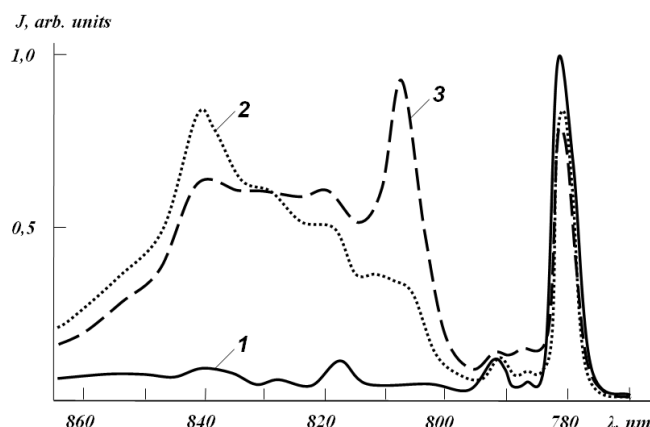


Fig. 1. Photoluminescence spectra of a CdTe crystal: before the indentation (1) and after the indentation (2, 3). The ratio of the exciting radiation intensities $I_3 / I_2 = 10^2$, the ratio of PL intensities $J_3 / J_2 = 5 \times 10^2$, face (001), $T=4.2 \text{ K}$

simultaneous clear observation of both bands is that of 33–55 K. In the temperature range 4.2–30 K, the dominant band is usually the one with a maximum at 1.536 eV (806 nm) at $T=4.2 \text{ K}$. A distinctive feature of the indicated bands of “dislocation” PL is their metastability: the bands practically disappear from the radiation spectra even after a relatively short-term (several hours) exposure of crystals at room temperature. At the same time, at lower temperatures of the storage of crystals ($T < 100 \text{ K}$), these bands remain in the radiation spectra for however long.

Another group of radiation lines that also arises due to the indentation of the crystal surface appears in the energy range 1.47–1.51 eV (843–821 nm). At a temperature higher than $T=4.2 \text{ K}$, the dominant band in this spectral region is usually the one with a maximum at 1.476 eV (841 nm). In the range $T=4.2 \div 100 \text{ K}$, one observes the bands at 1.47–1.51 eV (usually three bands). These radiation bands are stable and remain in the spectra even after the long storage of crystals at room temperature. It is also worth noting that, for the indented regions of the sample, together with the appearance of new (“dislocation”) PL bands, there takes place the noticeable suppression of the radiation bands of the initial CdTe samples: the radiation lines of exciton-impurity complexes (780.6 nm) and the impurity bands (860–950 nm). The latter are not presented in Fig. 1.

It is worth noting that, in Cd(Zn)Te crystals that represent a basic material of substrates for $\text{Cd}_x\text{Hg}_{1-x}\text{Te}$ epitaxial layers, we also discovered the new radiation bands possibly associated with the generation of dislocations (Fig. 2). Moreover, their positions in the PL spectrum generally appear to be shifted on the

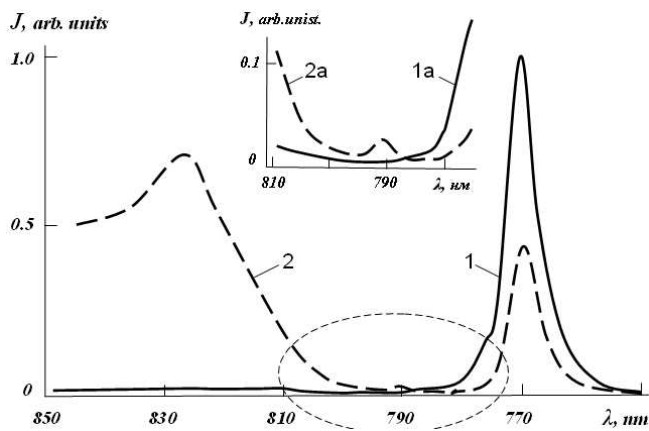


Fig. 2. Spectral distribution of PL of Cd(Zn)Te crystal before (solid curve) and after (dashed curve) the indentation. Face (001), $T=77$ K, Zn content — 6%. In the inset — the scaled-up fragment

wavelength scale with respect to the “dislocation” PL bands in CdTe: 792 and 827 nm, respectively.

Profiles of the spatial distribution of the PL intensity in “dislocation” bands. As was clarified from our first measurements, the profiles of the spatial distributions of the radiation intensity for all PL bands that belong to the same series appeared to be practically identical. That’s why, in order to record profiles, we chose the principal bands at 806 and 841 nm from each of the above series. As concerns the character of the plastic deformation, it is worth noting that CdTe monocrystals are deformed plastically according to the glide system $\langle 110 \rangle \{111\}$ [3,8]. Moreover, in the case of the indentation of the surface, the plastic deformation in CdTe crystals takes place in the form of the motion of dislocation semiloops [4,9].

Face (111). As seen from the pattern of the selective etching, after the application of a single prick with an indenter on (111) face, there arises a symmetric dislocation rosette near the indentation place. The rosette appears to be spatially triply degenerate (Fig. 3) and consists of six rays that determine the exits of the principal dislocations from dislocation semiloops onto the surface of the sample. In this case, one distinguishes the exits of α - and β -dislocations. The rays of the exits of α - and β -dislocations are located in parallel to one another. Due to a higher mobility of dislocations of the α -type, their rays appear to be more extensive (by a factor of 1.5–2) as compared to the rays of β -dislocations [2]. The scratches on surface (111) were applied along the direction $\langle 110 \rangle$ and in normal to it, i.e. along $\langle 1\bar{1}0 \rangle$.

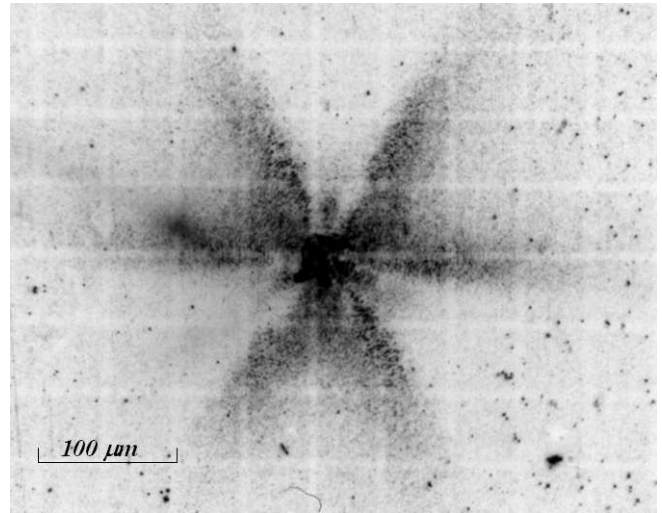


Fig. 3. Microphotography of the spatial distribution of dislocations close to the place of the indentation of (111) face. The load on a Vickers indenter — 10 g, $T=300$ K

For all the radiation bands including the initial ones, the profiles of the spatial distribution of PL in the vicinity of the scratch turned out to be weakly dependent on its direction, i.e. they are practically isotropic. Taking into account a high symmetry of the dislocation rosette on (111) surface, such a form of the profiles is completely clear. For both directions of the scratches, the profile of the 841-nm radiation band appeared to be wider than that of the 806-nm band by approximately a factor of two. That’s why, if we assume that both bands are of the dislocation origin, the 841-nm band should be related to the electronic states of more mobile α -dislocations, while the 806-nm band — to those of β -dislocations. However, such an assumption seems to be too premature, as the data only for (111) face are insufficient for a final conclusion.

Face (001). In order to clarify the pattern of the spatial distribution of dislocations in the case of the indentation of (001) surface, let’s first consider the arrangement of glide planes near a separate imprint of the indenter on this surface (Fig. 4). In the process of indentation, the crystalline material is displaced from the imprint region by means of the dislocation glide in the directions specified by a set of equivalent Burgers vectors. This results in the formation of the so-called glide branches (the bold points and lines in Fig. 4). In the middle of each glide branch, the polarity of an extra half-plane (that is, a half-plane bounded with either Cd or Te atoms) is determined by its crystallographic orientation and the direction of the Burgers vector of the dislocation.

In the case of the indentation of high-symmetry faces, the three-dimensional pattern of a spatial distribution of dislocation semiloops is usually divided into two systems. The “rosette” glide system includes the Burgers vectors parallel to the face plane (bold lines). The “tetrahedral” glide system corresponds to the Burgers vectors directed inward the crystal — bold points (Fig. 4). For example, the tetrahedral glide branch in Fig. 4, which is directed “to the right and to the plane of the figure”, will be bounded with two pairs of planes: $(\bar{1}\bar{1}\bar{1})\text{Te}$ and $(111)\text{Cd}$, $(\bar{1}\bar{1}\bar{1})\text{Cd}$ and $(\bar{1}\bar{1}\bar{1})\text{Te}$, respectively. That is, each “tetrahedral” glide branch contains extra half-planes bounded with both Cd and Te 60-degree dislocations (Cd(g)- and Te(g)-dislocations, respectively). They represent the principal dislocations of semiloops. Hereinafter, index (g) marks that the observed dislocations are glide ones.

As for branches of the “rosette” glide, it will develop at the expense of the glide of principal dislocations of either two Cs- or two Te-planes. That is, the extra half-planes will be bounded only by Cd or Te atoms, respectively. As is shown in [4], in the case of the indentation of (001) face, one pair of reflection symmetric rays of the rosette will be formed by the exits of the segments of 60-degree Te(g)-dislocations (or, in other words, α -dislocations), while the other pair of rays will be formed by the segments of 60-degree Cd(g)-dislocations (or β -dislocations) (in Fig. 4, the planes are marked with $(\bar{1}\bar{1}\bar{1})\text{Te}$, $(\bar{1}\bar{1}\bar{1})\text{Te}$ and $(\bar{1}\bar{1}\bar{1})\text{Cd}$, $(111)\text{Cd}$ indices, respectively). As a result, in the process of indentation of (001) face, the aggregates of the exits of Te(g)- and Cd(g)-dislocations appear to be spatially separated.

This implies that the direction of rectilinear scratches on (001) face is of significant importance. Indeed, the regions adjacent to the scratch will include the exits of either only Te(g)-dislocations on the crystal surface $+/- \langle 1\bar{1}0 \rangle$ direction) or only Cd(g)-dislocations ($+/- \langle 110 \rangle$ direction). That’s why in order to identify the types of defects, whose generation results in the appearance of the corresponding bands of the “dislocation” radiation in PL spectra in CdTe, the scratches were applied to (001) surface exactly in the above-mentioned directions. The directions $\langle 110 \rangle$ and $\langle 1\bar{1}0 \rangle$ on the sample were determined by the etch patterns [10]. Based on the above, it was worth expecting a distinct anisotropy of the profiles of the spatial distribution of the radiation intensity in the 841- and 806-nm PL bands, but only in the case where the both bands are indeed directly associated with the states of either Te(g) or Cd(g) dislocations.

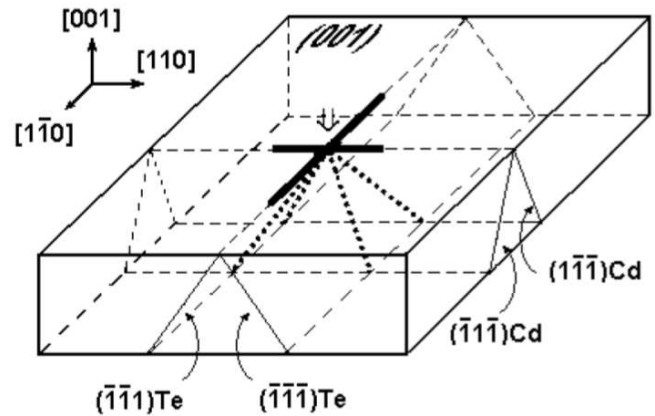


Fig. 4. Diagram of the spatial distribution of the glide planes in the case of the indentation of (001) face. The large arrow at the center indicates the indentation place. The rosette of the surface distribution of dislocations is shown with continuous bold lines. The thin arrows mark the planes that correspond to the systems of rosette and tetrahedral glides. The directions of the development of the tetrahedral glide are marked with thick points

As one can see from Fig. 5, the spatial distribution of the intensity of the 841-nm radiation band really manifests a well-defined anisotropy. The half-widths of the profiles for two mutually perpendicular directions differ by several times. At the same time, the anisotropy in the profiles of the 806-nm band is practically absent. One can also see (the inset in Fig. 5) that the width of the profiles considerably exceeds the width of the scratch itself (also taking into account the region of microcracks). This testifies to the fact that “dislocation” PL isn’t related to any violation of the integrity of the crystal.

Comparing the diagram of the dislocation structure in Fig. 4 with the fact that the half-width of the profile of the 841-nm band for the $\langle 1\bar{1}0 \rangle$ direction of the scratch exceeds that for the $\langle 110 \rangle$ direction by several times, one can make an unambiguous conclusion that the 841-nm band is directly related to the electronic states of Te(g)-dislocations. Such a result also coincides with the conclusions made in works [4,5]. The width of the intensity profiles for the 820-nm and 830-nm radiation bands has the same orientation dependence as that for the 841-nm band. This testifies to the fact that all the radiation bands that form the given series belong to electronic states of the same type of defects, namely to Te(g)-dislocations.

The absence of a noticeable anisotropy of the radiation intensity profiles in the 806-nm band is the evidence for the fact that this band cannot be related

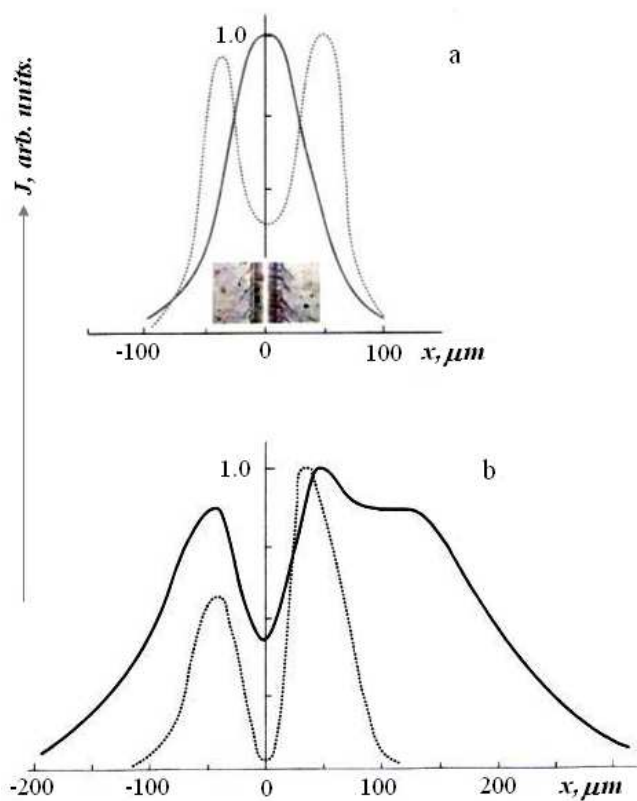


Fig. 5. Profiles of the spatial distribution of the PL radiation intensity in the 841-nm (solid curve) and 806-nm (dotted curve) bands on (001) face: *a* — for the scratch in the $\langle 110 \rangle$ direction, *b* — for the scratch in the $\langle 1\bar{1}0 \rangle$ direction. In the inset — optical microphotography of the region of the scratch in the $\langle 110 \rangle$ direction on the scale of the *X* axis in (001) face

to the electronic states of either Cd(g)- or Te(g)-dislocations. Indeed, according to the considered model (see Fig. 4), a distinct anisotropy of the profiles must be observed in the both cases, but it is absent in the experiments. Taking into account the metastability of the 806-nm band as well, it is worth supposing that the 806-nm radiation cannot be directly related to the states of the dislocation core (as it turns out for the 841-nm band). It should be associated with the electronic states of less stable defects that arise due to the motion of dislocations. Moreover, the indicated defects also cannot be elementary point defects, as the 806-nm radiation in CdTe is observed only after the low-temperature motion of dislocations. It doesn't arise due to any other influences on the crystal which generate point defects (for example, due to the bombardment of the crystal with high-energy particles). The metastable states can be related to some ordered structures of point defects. Such structures are formed as a result of

the motion of dislocations with steps, as was shown in [11, 12].

Figure 5 contains another important information that allows one to make a conclusion concerning the type of dislocations, whose motion results in the generation of the indicated metastable defects responsible for the 806-nm radiation. Indeed, for one of the directions of the scratch, namely for the $\langle 110 \rangle$ one, the half-width of the profile of the 841-nm band appears to be much narrower than that of the 806-nm band profile. It's obvious that the point defects generated by mobile dislocations in no way can reach the part of the crystal, where the indicated dislocations couldn't get to. Such a statement is even more correct in the case of low temperatures. That's why one can conclude that the defects responsible for the 806-nm radiation can by no means be related to the motion of Te(g)-dislocations. Thus, the 806-nm radiation should be associated with the structure of defects generated due to the glide of dislocation semiloops with principal Cd(g)-dislocations.

Let's consider the mechanism of the "ordered" generation of defects during the motion of dislocations in more details. The glide processes of dislocations in CdTe take place by means of the motion of dislocation semiloops in the Peierls relief in the $\langle 1\bar{1}0 \rangle \{111\}$ glide system. Each semiloop consists of at least one screw segment connected with two segments of the edge dislocation. These segments represent either 60-degree Te(g)- or 60-degree Cd(g)-dislocations. All dislocations usually originate in the same region of the crystal — close to the prick of an indenter. When the dislocation loops diverge in various equivalent directions under the action of a loading, they intersect and form steps on one another. As a matter of fact, such an intersection becomes possible only in the spatial region close to the prick of an indenter, i.e. in the central area of the dislocation rosette.

As is known, the motion of screw dislocations with steps represents an effective mechanism of formation of point defects. If such screw dislocation moves, the creep of a step along the way of its motion results in the generation of the chains of point defects: vacancies and interstitial atoms. In this case, the number of defects formed due to a single creep of the step (by the length of the lattice constant) is equal to the number of atoms in the unit cell of the crystal.

Thus, due to the generation and the motion of dislocations in crystals, along with proper dislocation electronic states (that is, those corresponding directly to the dislocation core), there also arise other states of defects. They are associated with some ordered

structures — the chains of point defects. The latter are formed during the motion of screw dislocations with steps. It is obvious that, from this viewpoint, the most effective dislocations are those with a considerable number of steps, that is the least mobile dislocations. As a result, the defects are mainly generated close to the center of the dislocation rosette, where the dislocation mobility anisotropy is essentially distorted. It is the spatial distribution of the chains of point defects close to the place of the indenter prick that specifies the width of the profiles and, respectively, the spatial orientation dependence of the 806-nm band. That's why one should expect a practically isotropic distribution of the indicated defects, which completely agrees with the absence of a noticeable anisotropy in the profiles of the 806-nm band. As follows from the presented model, for the intensity of the 806-nm band on a face of the (001) type, the anisotropy must be practically absent, which agrees well with the experimental data.

According to the model of the quasio-one-dimensional chains of defects formed by the steps of dislocations in A^2B^6 crystals, the radiative transitions via their states represent the radiative annihilation of excitons connected with quasio-one-dimensional structures — chains [11]. Another evidence of the exciton nature of the 806-nm radiation band is the same (with regard for an experimental error) superlinear dependence of the intensity of the 806-nm band and the radiation line of a bounded exciton (780 nm) on the excitation power. At the same time, for the 841-nm band, this dependence has a sublinear character typical of the radiative recombination via impurity states. The different dependences on the radiation intensity for two series of “dislocation” PL can be well seen from the form of the PL spectrum of CdTe crystals with dislocations depending on the excitation intensity. Another feature of the 806-nm band — metastability — is conditioned by a low binding energy in the middle of the chain structure [12].

As was mentioned above, in the region of indentation of the CdTe surface, along with the appearance of new bands of “dislocation” PL in the radiation spectrum, the suppression of the initial radiation bands occurs: the impurity band (880 nm) and that related to exciton-impurity complexes (780 nm). In this case, the overall quantum yield of radiation from the indented region of the sample essentially decreases. This testifies to the fact that the suppression of the initial bands doesn't represent a direct consequence of the appearance of a new radiation channel in the form of “dislocation” PL (that is, the “transfer” of radiation from one spectral

region to another). On the contrary, this denotes the generation of some additional centers of nonradiative recombination due to the motion of dislocations, whose appearance results in a decrease of the summary quantum yield of the radiation of a crystal. In this connection, it's interesting to compare the profiles of the spatial distribution of the intensity of the initial radiation bands with the profiles of new “dislocation” PL bands. The half-width of the profiles of the initial bands appeared to be much narrower than the intensity profile of the 841-nm dislocation radiation and, at the same time, close to the half-width of the profile of the 806-nm band. The spatial distribution of the radiation of the initial bands turns out to be practically isotropic similarly to that for the 806-nm band. This result becomes clear based on the assumption that the additional nonradiative centers of recombination are not directly the states of the dislocation core but point defects (vacancies, interstitial sites, and their complexes) generated due to the motion of dislocations. The density of such defects is evidently maximal in the region of intersection of dislocations, i.e. in the immediate vicinity to the place of indentation.

4. Conclusions

The macroscopic plastic deformation in CdTe and Cd(Zn)Te crystals results in essential changes in the spectra of radiative recombination, which is connected with the formation of the additional levels of defects in the forbidden band. In the spectra, there appear new radiation bands — “dislocation” PL — that consist of two series of radiation bands with the principal bands at 806 and 841 nm ($T=4.2$ K). They have no analogs in CdTe under any other influences on the crystal that cause the appearance of proper defects. We have obtained the profiles of the spatial distribution of the radiation intensity for “dislocation” bands on (001) and (111) surfaces. Comparing these profiles with the diagrams of glide systems as well as with the configuration of dislocations, we conclude that the 841-nm series is directly related to the electronic states of 60-degree Te(g) dislocations (α -dislocations). At the same time, the 806-nm series can be associated with the states of the ordered structures (quasio-one-dimensional chains) of point defects. Quasio-one-dimensional structures are generated due to the motion of screw dislocations with steps that follow principal Cd(g)-dislocations (β -dislocations). The radiative transitions on quasio-one-dimensional structures are fulfilled with the help of excitons bounded to them.

1. H. Nakagava, K. Maeda, and S. Takeuchi, *J. Phys. Soc. Jpn.* **49**, 1909 (1980).
2. S.V. Lubenets and L.V. Fomenko, *Fiz. Tverd. Tela* **33**, 145 (1989).
3. N.I. Tarbaev, J. Schreiber, and G.A. Shepel'skii, *Fiz. Tverd. Tela* **31**, 1348 (1989).
4. H.S. Leipner, J. Schreiber, H. Unievski, and S.Hildebrant. *Scanning Microscopy* **11**, 149 (1998).
5. J. Schreiber, L. Yuring, H. Unievski, S. Hildebrant, and H.S.Leipner, *Phys. status solidi (a)* **171**, 89 (1999).
6. V.N. Babentsov, S.I. Gorban', E.A. Sal'kov, and N.I. Tarbaev, *Fiz. Tekhn. Polupr.* **21**, 1043 (1987).
7. C. Diaz-Guerra, U. Pal, P. Fernandes, and J. Piqueras. *Phys. status solidi (a)* **147**, 75 (1995).
8. A. Orlova and B. Sieber, *Acta met.* **32**, 1045 (1984).
9. E. Hall and J.B. Vander-Sande, *J. Amer. Ceram. Soc.* **61**, 417 (1978).
10. H. Iwanaga, A. Tomizuka, N. Shibata, and M. Mochezuki, *J. Cryst. Growth* **74**, 113 (1986).
11. N.I. Tarbaev G.A. Shepel'skii, and E.A. Sal'kov, *Pis'ma Zh. Eksp. Teor. Fiz.* **66**, 639 (1997).
12. N.I. Tarbaev and G.A. Shepel'skii, *Fiz. Tekhn. Polupr.* **32**, 646 (1998).

Received 13.09.06.

Translated from Ukrainian by H.G. Kalyuzhna

СТРУКТУРА ДИСЛОКАЦІЙ І “ДИСЛОКАЦІЙНА”
ФОТОЛЮМІНЕСЦЕНЦІЯ В КРИСТАЛАХ
ТЕЛУРИДУ КАДМІЮ

В.А. Бойко, М.І. Тарбаєв, Г.А. Шепельський

Резюме

Генерація дислокацій в кристалах CdTe та Cd(Zn)Te зумовлює появу в спектрах випромінювальної рекомбінації нових смуг — “дислокаційної” фотолюмнісценції. Із порівняння просторового розподілу інтенсивності випромінювання для різних смуг випромінювання на гранях (111) та (001) з кристалографічною структурою дислокацій ідентифіковано типи дефектів, що відповідають за “дислокаційну” фотолюмнісценцію.